Proceedings of the Canadian Society for Mechanical Engineering International Congress 2022
CSME Congress 2022
June 5-8, 2022, Edmonton, AB, Canada

Validation of a Numerical Model for Reciprocating Thermodynamic Machines by Examining Heat Transfer in a Low Temperature Difference Stirling Engine

Matthias Lottmann[1], David S. Nobes[1]*
[1]Department of Mechanical Engineering, University of Alberta, Edmonton, AB, Canada
*dnobes@ualberta.ca

Abstract—A third order two-dimensional numerical model for reciprocating thermodynamic machines is validated using a low temperature difference Stirling engine with 15 Watt shaft power and source and sink temperatures of 150 °C and 5 °C. The work is limited to the thermodynamic model at steady state. The deviation for indicated work between model and experiment is below 30 % and varies significantly with mean pressure and engine speed. Likely sources of error are differences in heat exchanger geometry between experiment and model due to current model limitations, and empirical correlations for heat transfer and flow friction based on Reynolds number (Re) used by the model. Analyzing the data in terms of heat exchanger Re reveals a strong linear relationship between model error and Re. Building on the results of this study, the model can be used in similar applications, continuously validated, improved and expanded as its source code is openly available.

Keywords - model; validation; experimental; thermodynamic; heat transfer; Stirling; geothermal; waste heat

I. INTRODUCTION

The technological and ecological push towards renewable energy has increased the interest in utilization of unconventional energy resources that have often been evaluated as uneconomical. One example is low temperature (LT) heat which exists abundantly in the province of Alberta in the form of industrial waste heat and geothermal heat. LT in this context refers to source temperatures below 150 °C. About 388 GW of thermal energy could be reasonably extracted from geothermal reservoirs in Alberta [1], which is enough to cover the peak electricity demand [2] of the province if converted at 3 % efficiency.

Stirling engines are a type of heat engine that can utilize heat from any external source to produce power. In contrast to conventional prime movers that use turbomachinery, they can work efficiently at a small power scale, be exceptionally low-maintenance and durable, and even be designed as free-piston machines that operate with negligible mechanical friction and wear. This makes Low Temperature Difference Stirling Engines (LTDSEs) a technology with great potential to utilize a so far unused renewable resource if they can be proven economically viable despite the thermodynamic limit to power density for any machine working with a small temperature difference.

The development of these complex thermodynamic machines is highly iterative and relies on experiments because little research exists on large scale LTDSEs. The design process could be greatly facilitated by a mathematical model that would predict performance of LTDSE numerically. In Stirling machine research, models are commonly categorized into orders of complexity. First order models are analytical equation sets that assume a greatly simplified behavior of the working gas. The Schmidt model [3], for example, assumes working spaces to be isothermal and can be solved in closed form.

Second order models calculate energy losses that occur in a real engine, such as flow friction, separately and apply them to the results of an idealized model. An example is the SIMPLE model by Urieli and Berchowitz [4] which is based on an adiabatic analysis. These models can give estimates for the performance of an engine concept without requiring detailed knowledge of its geometry, which is helpful in the early design stage of a Stirling machine.

The power output of LT engines is greatly affected by energy losses through flow friction and heat conduction. Predicting these requires more detailed modeling of all processes affecting the working gas, solid conduction and mechanical friction. This is achieved by third order models through discretization of the engine geometry into a network of nodes. An established model of this kind is Sage [5], which solves a one-dimensional representation of a reciprocating machine at steady state. However, it is not validated at LT, cannot model transient cases and is not openly available to researchers.

To fill this gap and accelerate the development of LT engines, MSPM [6] was developed at the University of Alberta. The goal of this two-dimensional MATLAB-based model is to simulate the complete thermodynamic and mechanical system of reciprocating machines, especially aimed at the LT regime.

The ongoing validation of the model with experimental data is the subject of this paper. Currently the focus is on the thermodynamic side of the model for predictions of working gas pressure, temperatures, heat flows and flow friction, at steady state. The mechanical and transient parts of the model require

Sponsors:
Natural Sciences and Engineering Research Council (NSERC) of Canada,
Alberta Innovates Energy and Environmental Solutions,
University of Alberta Future Energy Systems

further testing and will be validated at a later stage. The primary goal of this validation, apart from assessing the level of discrepancy between the model in its current state and experiments, is to find trends in the model accuracy depending on operating points that reveal weaknesses in the model assumptions and equations which can then become the focus of further work to improve the model. The comparison will be made against experimental data from a LTDSE prototype developed in the author's research group.

II. The Stirling Cycle

Knowledge of the basic processes occurring in a Stirling engine is required to understand the critical role heat transfer plays in its performance. More in-depth reviews of Stirling cycle theory and components can be found in [6], [7]. A Stirling engine is a closed cycle reciprocating heat engine that draws thermal energy from a heat source, converts some of it into mechanical work, and rejects remaining heat to a heat sink at a lower temperature. Figure 1 shows the following processes in a characteristic Stirling cycle indicator diagram.

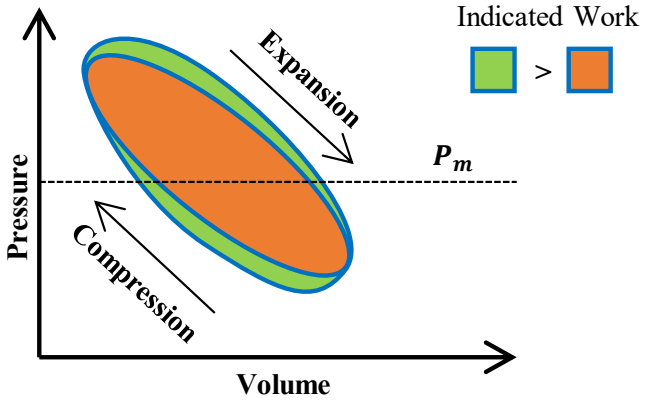

Figure 1: Two Stirling indicator plots with different indicated work

A constant mass of working gas (in this case air) goes through a cycle of heating and cooling by moving back and forth through a set of heat exchangers (source/sink). The gas temperature alternates between hot and cold, which causes an oscillation of pressure in the working space. During high pressure the engine volume is expanded and during low pressure it is compressed. During both times, work is extracted from the gas. The net work output per cycle is called the indicated work, W_{ind}, and is equal to the area enclosed by the indicator diagram.

The regenerator is a component located between the hot and cold heat exchangers and acts like a heat 'sponge'. It stores thermal energy from one cycle to the following by absorbing and releasing heat, thereby reducing the load on the heat exchangers. Composed of high surface area material such as steel wool, it contributes significantly to heat transfer and flow friction.

The gas displacement and volume changes are usually caused by reciprocating pistons, which are in turn linked to a mechanism that controls the piston motion and transfers mechanical work between them and a flywheel, much like any other piston machine. Shaft power is used to quantify the net output achieved by the entire engine system, including the mechanical losses which are currently not represented in the MSPM model.

Since only the thermodynamic model is of interest, an appropriate measure for validation is the indicator diagram. Its area or W_{ind} is commonly used to compare Stirling machines and models. However, two indicator diagrams with equal area could have dissimilar shapes. Shape is a much stronger measure of performance for the thermodynamic model because it reflects the gas pressure at each point in the cycle. Therefore, both shape and area of the indicator diagram will be the main criteria to compare experiment and model results.

Insight into the performance of the heat exchangers and regenerator, i.e. the amount of heat transferred to and from the gas per cycle, can be gained by inspecting the vertical 'height' of the indicator diagram at any point on the horizontal axis. This pressure difference between two points with equal volume is a result of the temperature change caused by heat addition and rejection. The deviation between the two curves shown in Figure 1 is an example for this relation. One of them has a greater pressure difference and therefore W_{ind} than the other.

III. Desription of the Model

MSPM ('Modular Single Phase Model') is a numerical code published in 2021 [6] that aims to simulate the behavior of an entire thermodynamic system with reciprocating components. It is comprised of a thermodynamic part which solves gas flow rates, heat transfer, conduction, flow friction, turbulence, and a mechanical part that can model the motion of mechanical linkages with friction and inertia which result from the forces determined from the thermodynamic side. The user creates a two-dimensional geometry from modular blocks in a GUI, which is discretized into a nodal network on which governing equations are solved. This allows it to work with arbitrary geometries as long as they can be represented by two-dimensional axisymmetric structures, which most piston machines are.

The following assumptions are central to the model:

- Two-dimensional geometry, where nodes represent cylindrical or annular elements. All properties are averaged along the circumferential direction.
- One-dimensional gas flow
- Gas properties follow the ideal gas law
- No contact resistance between nodes, this might lead to overestimated heat transfer
- Neglecting radiation, gas inertia, gravity
- Matrix flow assumed to be always fully developed, which might cause inaccuracy for certain heat exchanger geometries

IV. Description of the Engine and Experiment

Experimental data is obtained from the 'Raphael' engine shown in a cross section in Figure 2. It is a gamma type engine with a total working space volume of around 4.7 liters that produces 15 Watts of shaft power from source / sink temperatures of 150 / 5 °C. The design is based on that of the ST05G-CNC which is no longer publicly available but was also used by Speer [8]. Modifications were made to adapt it to a lower

temperature difference, most notably a larger displacer cylinder bore and a two-fold increase of heat exchanger volume and surface area [9].

Relevant for this work is the geometry of the heat exchangers. They are located in an annulus outside of the displacer piston and have longitudinal fins parallel to the gas path. The gas flows through rectangular channels between the fins. Around the outside of the annulus lies the source channel through which heat transfer liquids flows circumferentially, conducting heat to the gas on the inside. Relevant parameters are listed in Table 1.

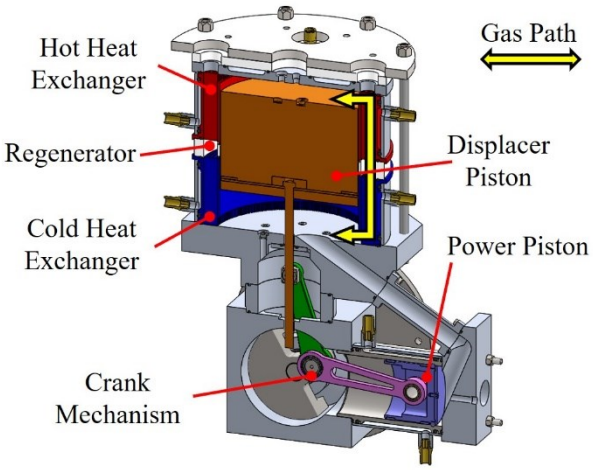

Figure 2: Cross section of engine solid model showing working spaces

TABLE I. PROPERTIES OF 'RAPHAEL' ENGINE RELATING TO THERMODYNAMIC MODEL

Displacer piston swept volume	2.4 L
Power piston swept volume	0.4 L
Displacer piston diameter	200 mm
Heat exchanger gas channel dimensions	20 mm × 1 mm 287 channels
Heat exchanger depth (gas path length)	96 mm
Regenerator ID, OD, depth (gas path length)	207 mm, 247 mm, 25.4 mm
Regenerator material	Random polyester fibers Diameter 0.1 mm Porosity 96 %
Heat exchanger flow velocity at 240 rpm	Avg. 3.3 m/s, Max 5.1 m/s
Hot side gas temperature range	85 – 120 °C
Cold side gas temperature range	20 – 35 °C

Achieving 'true' steady state conditions is difficult as due to its thermal mass, the engine takes several hours to reach complete thermal equilibrium after changing the operating point. It is critical however when comparing to a model that assumes perfect steady state. A wait time of one hour after startup and ten minutes between operating points before acquiring data was determined reasonable from observing transient data.

Data was recorded with a computer controlled DAQ system. The pressure data used for all results was measured at the power piston cylinder using a diaphragm static pressure sensor combined with a piezoelectric dynamic pressure sensor. All pressures referred to are gauge pressure to atmosphere as this is how experiment data is recorded. The performance of heat engines depends on the absolute pressure in the working space because it relates to the mass of working gas in the system. For that reason, the model requires the absolute mean pressure as an input, which is calculated from the measured gauge pressure and local atmospheric pressure at the time of the experiment.

This work analyzes the heat transfer related accuracy of the model but does not deal with flow friction. Since the experiment data lacks a measurement of pressure on both sides of the heat exchangers, pressure drop from friction cannot be quantified. Data with an additional pressure sensor will be recorded in future work to fill this gap.

V. VALIDATION RESULTS AND DISCUSSION

Four experimental data sets were collected, each at a different engine mean pressure, P_m = 200, 350, 400 and 450 kPa. Each data set contains between 18 and 29 data points that cover the full range of engine speeds. This is from maximum speed with no load torque applied to the minimum speed and highest load torque at which the engine could operate without stalling.

A. *Indicator Diagram – Area and Shape*

Figure 3 shows indicator diagrams obtained at the lowest and highest P_m and speed, respectively. The plots from experiment and model have been shifted to share equal P_m and volume. This allows the calculation of the overlapping area between the plots, which represents the degree to which their shapes are similar.

Figure 3(a) shows that the model significantly underestimates heat flow at P_m = 200 kPa and low speed as the experiment curve is taller and has a greater area than the model curve. However, at high speed Figure 3(b) the experimental indicator area is much smaller while the model result is similar, though still slightly smaller, resulting in an overlap of over 90 %.

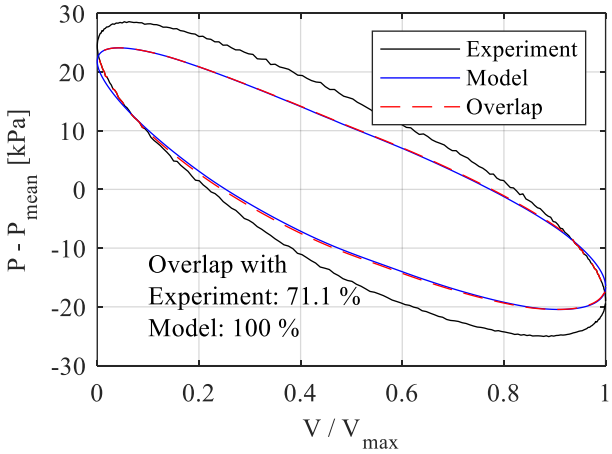

(a) P_m = 200 kPa, min Speed = 116 rpm

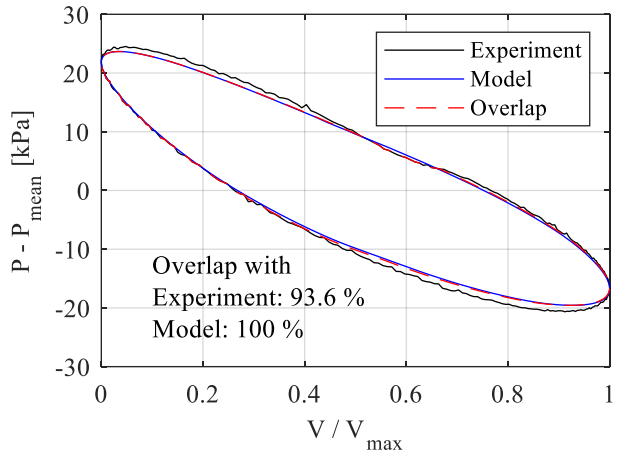

(b) P_m = 200 kPa, max Speed = 240 rpm

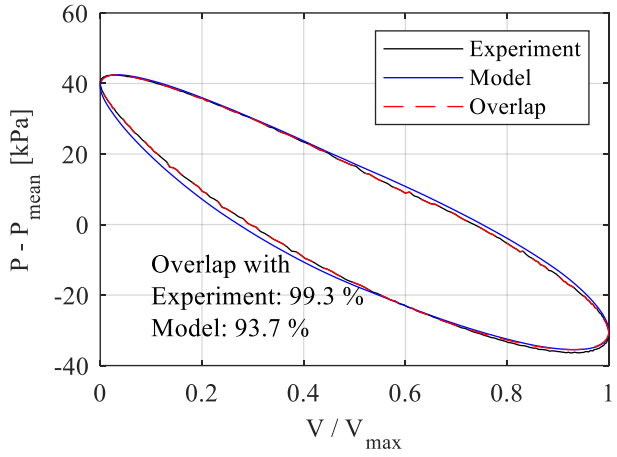

(c) P_m = 450 kPa, min Speed = 125 rpm

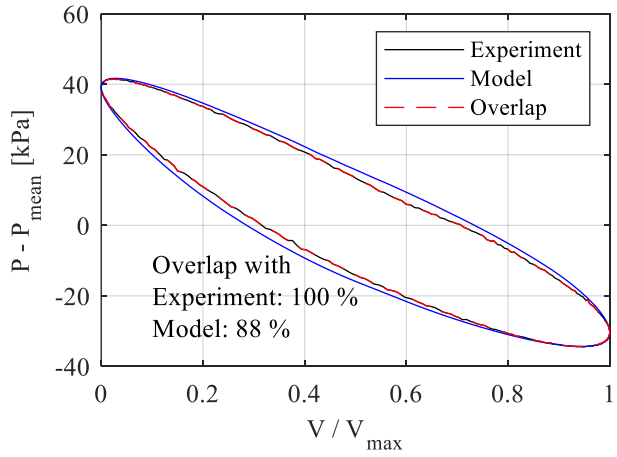

(d) P_m = 450 kPa, max Speed = 169 rpm

Figure 3: Indicator diagrams from experiment and model, with overlap area and overlap percentage relative to indicator areas. For P_m = 200 kPa (a,b) and 450 kPa (c,d), each at minimum (a,c) and maximum (b,d) speed.

Moving to P_m = 450 kPa in Figure 3 (c)-(d), a strong agreement around 90 % is observed for both high and low speeds. But in contrast to the low-pressure case, the model is now overpredicting heat transfer slightly as its curve mostly surrounds the experiment curve. This deviation is more pronounced at higher speeds, although the speed difference between load-free and stalling is relatively smaller at high pressure. This is due to the engine reaching flow friction and heat transfer limits more quickly as a result of the Reynolds number increasing with pressure.

B. Model Accuracy vs. Pressure and Speed

The trends gathered from the sample indicator diagrams are confirmed by the combined data of all four data sets. Figure 4 plots the indicator overlap percentage of all data points with speed. The absolute values of W_{ind} from experiment and model results is shown in Figure 5. To facilitate comparison and analyze how the deviation changes with engine speed and P_m, the deviation of between W_{ind} from model and experiment is displayed in Figure 6. It can be expected that this deviation shows similar trends to the overlap ratio in Figure 4 since both represent a relative error.

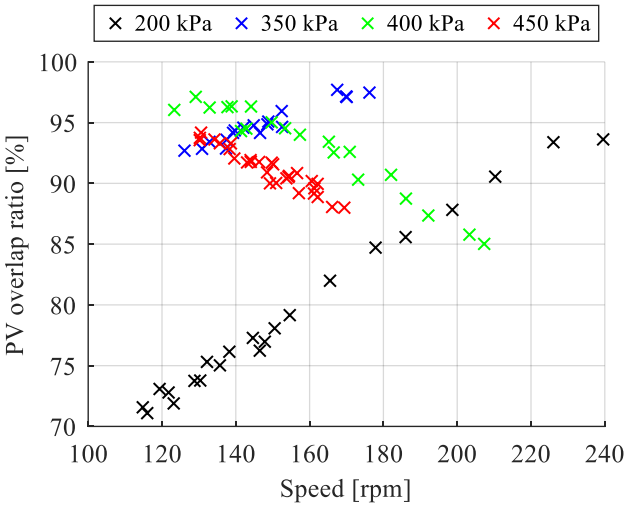

Figure 4: Indicator diagram overlap ratio vs. speed and P_m

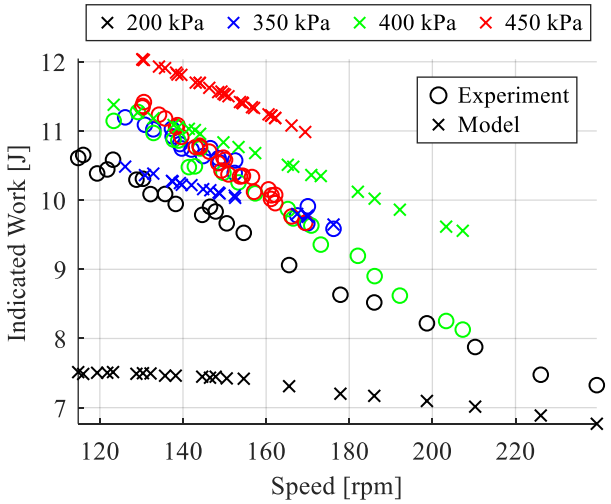

Figure 5: Indicated work vs. speed and P_m

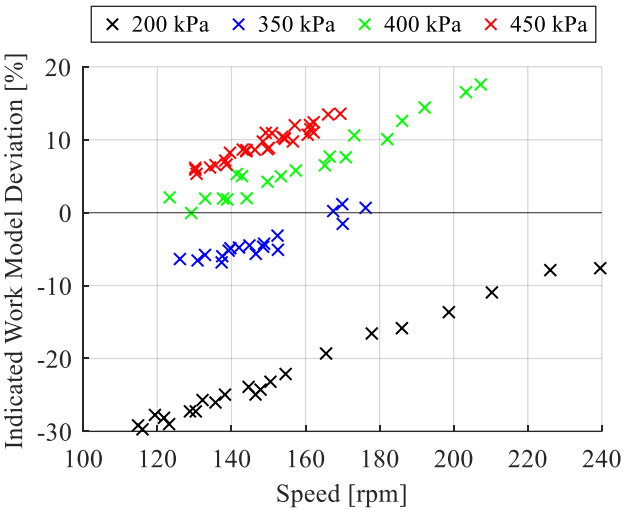

Figure 6: Indicated work deviation of model from experiment vs. speed and P_m

Regarding the overall accuracy of the thermodynamic model predictions, Figure 4 and Figure 6 show that the relative model error in terms of the indicator diagram is within 30 % for $P_m = 200$ kPa and less than 15 % for the higher P_m cases. This can be seen as a strong level of agreement considering the limitations of the model code and the high level of simplification between the real engine and its model representation used for these results, as discussed in Section III. Deviation below 15% indicates that the model can make relatively accurate predictions at least within some range of operating points, and could be used to inform the design of heat exchangers for oscillating flow and to improve heat transfer in existing engines.

The model was previously validated by its author against a LT engine at 95 °C source temperature and atmospheric pressure and achieved a maximum and average error of 35 % and 22 % respectively [6]. Though the method of calculating error was different here, it can be said for certain that the model performed similarly or better in this present work.

The way W_{ind} varies depending on P_m and speed as shown in Figure 5 reveals two trends. Firstly, W_{ind} always decreases with increasing speed at a constant P_m. This is expected because a higher speed implies a shorter time in which the gas passes through the heat exchangers, which reduces the temperature change of the gas since the heat exchangers are not isothermal. However, the experiment sees a steeper decline of W_{ind} with respect to speed, and it seems likely that for any P_m the two curves would meet at some speed. For the data sets with $P_m = 200$ kPa and 450 kPa this speed lies outside of the range of the experiment in which the engine runs on its own power.

The model also predicts W_{ind} to always increase when P_m is increased at a constant speed. This is also expected since along with P_m increases the mass of gas in the working space. As long as the heat exchangers are capable of exchanging a greater amount of energy with a greater mass of gas, the pressure swing and W_{ind} will increase. However, the experimental data shows that there is almost no change in W_{ind} between $P_m = 350$ kPa and 450 kPa since these data points fall onto one line in Figure 5.

C. Heat Transfer Limit and Heat Flow Path

These trends indicate that the model does not correctly represent the effect of the thermal limit to heat transfer in the heat exchangers which prevents the real engine from producing more work at high pressure and speed. Pressure and speed affect heat transfer in the same way through their proportional relationship to the Reynolds number (Re), which characterizes fluid flow in the heat exchanger matrix:

$$Re \propto \rho \times U \propto P \times f \quad (1)$$

Density, ρ, is proportional to pressure, P, through the ideal gas law and the bulk flow velocity, U, in the heat exchangers at any time is proportional to the engine frequency or speed, f. For a real heat exchanger there will be some Re at which a heat transfer limit is reached, and further increase of Re no longer notably increases the heat flow rate. This limit is caused by a series of thermal resistances which the heat must pass through between the heat source or sink and the fluid being heated or cooled. In the case of the 'Raphael' engine heat exchangers these resistances are:

- Convection between heat transfer liquid and wall of source channel. The liquid can be considered an isothermal heat source / sink.
- Solid conduction between source channel wall and heat exchange surface of gas channel and fins.
- Convection between heat exchange surface and gas.

The model representation of the heat exchangers that was used for this study is simplified considerably in that it does not consider the convection heat transfer between source liquid and wall. This is due to a model limitation that currently permits heat sources only in the form of isothermal solid bodies that transfer heat perfectly by pure conduction. CFD simulations have shown that this convection resistance represents a major bottle neck in the heat flow path. By omitting it, the model heat exchanger may be capable of substantially higher heat flow rates before running into a heat transfer limit. This inconsistency is likely the main reason why the model predicts W_{ind} to increase further with Re while the experiment indicates a heat transfer limit.

Another indicator for the heat transfer limit is the fact that the highest shaft power in all experiments was measured close to minimum speed. This suggests that this engine is limited significantly by heat transfer performance and flow friction, both of which prevent shaft power from increasing at higher speeds.

D. Model Accuracy vs. Reynolds Number

In Figure 6 all data sets show linear relations with similar slopes between the W_{ind} deviation and speed. This can be reduced into a single relationship when viewed as a function of the average Re in the heat exchangers as shown in Figure 7. It confirms the strong link between heat transfer, and therefore model accuracy, to Re. This is expected because the model obtains the parameters that affect thermodynamic processes, namely Nusselt number and Darcy friction factor, from empirical correlations that are functions of Re [6]. These correlations play a critical role in predicting heat transfer and flow friction, which translate into the Re-dependent behavior observed in the model results. To improve model accuracy, the

correlations must be checked for validity and adjusted against experimental data relative to Re.

Figure 7 also shows that all data points have an average Re in the laminar regime ($Re < 2300$). Further validation should examine cases with higher Re where the turbulence model of MSPM would play a role.

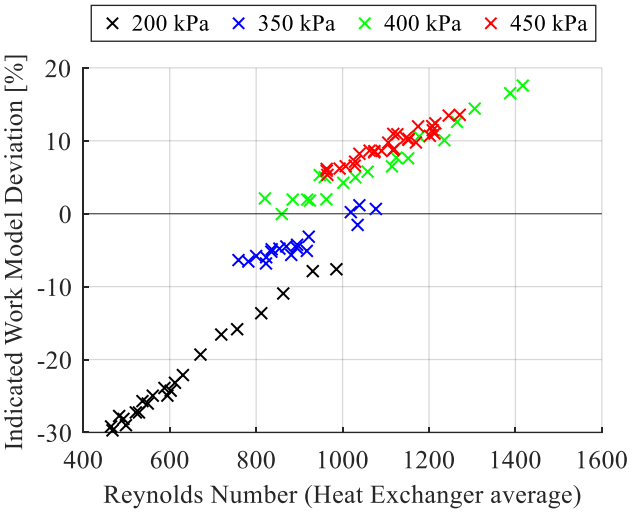

Figure 7: Indicated work deviation of model from experiment vs Reynolds number

E. *Thermal Efficiency*

As a common measure in the Stirling literature, thermal indicated efficiency is shown in Figure 8, calculated from W_{ind}, speed and heat flow rate supplied to the heat source. The model does not reflect the trend of decreasing efficiency with increasing P_m observed experimentally. as it predicts W_{ind} to increase with P_m. However, the trend of efficiency vs. speed is predicted quite closely for all curves, suggesting that the systematic error may be from the discrepancy in the heat flow path in the model as discussed in Section V C.

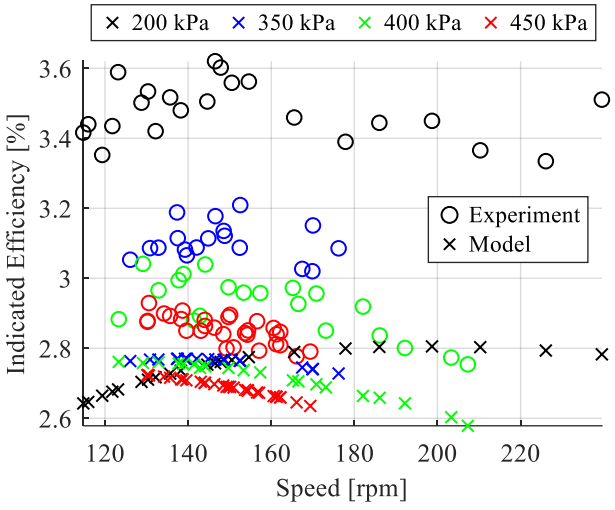

Figure 8: Indicated efficiency vs. speed and P_m

VI. Conclusions

Validation of the MSPM model against data from a LT Stirling engine at steady state has revealed that the model error in predicting the area and shape of the indicator diagram is below 30 % for P_m = 200 kPa and below 15 % for $P_m > 350$ kPa. The error varies significantly with P_m and engine speed.

Likely sources of error in the thermodynamic model were identified: The heat transfer path between an isothermal source and the working gas must be modeled more accurately to predict heat transfer limits. Also, the model error in W_{ind} depends strongly on Re in the heat exchangers. This may be linked to assumptions and empirical correlations used by the model based on Re. The model assumptions and correlations must be tested and modified in terms of Re. Also, higher Re scenarios with turbulence in the heat exchanger flow should be included in the analysis.

MSPM is written in MATLAB, features a GUI and its open-source code is openly available to researchers, which makes it highly flexible and accessible compared to other models for reciprocating thermodynamic machines. The results presented here measure the accuracy of MSPM's thermodynamic model as a function of Re, which can be applied directly to other applications with low pressure, temperature and Re. This is intended as an invitation for researchers to continue validating and improving the model and build on its potential.

References

[1] Canadian Geothermal Energy Association, "Canadian National Geothermal Database and Territorial Resource Estimate Maps: Alberta." https://www.cangea.ca/albertageothermal.html (accessed Feb. 10, 2022).

[2] S. Rieger, "Heat wave pushes Alberta past record high electricity demand." https://www.cbc.ca/news/canada/calgary/calgary-electricity-demand-1.6083483 (accessed Feb. 10, 2022).

[3] G. Schmidt, "Theorie der geschlossenen Lehmann'schen Maschine," *Zeitschrift des Vereines Deutscher Ingenieure*, vol. 15, no. 1, 1871.

[4] I. Urieli, "Stirling Cycle Machine Analysis." https://www.ohio.edu/mechanical/stirling/index.html (accessed Feb. 10, 2022).

[5] D. Gedeon, "Sage User's Guide." http://www.sageofathens.com/Documents/SageStlxHyperlinked.pdf (accessed Feb. 10, 2022).

[6] S. M. W. Middleton, "A Modular Numerical Model for Stirling Engines and Single-Phase Thermodynamic Machines," Thesis, University of Alberta, 2021. doi: https://doi.org/10.7939/r3-x8qd-p159.

[7] C. D. West, *Principles and applications of Stirling engines*. New York: Van Nostrand Reinhold, 1986.

[8] C. P. Speer, "Modifications to Reduce the Minimum Thermal Source Temperature of the ST05G-CNC Stirling Engine," Thesis, University of Alberta, 2018. doi: https://doi.org/10.7939/R3930P94X.

[9] C. Speer, Personal Conversation, 2021.